ISBN: 978-3-95450-168-7 doi:10.18429/JACoW-IPAC2015-MOPWI031

MICROWAVE MODELING FOR ELECTRON CLOUD DENSITY MEASUREMENTS AT CESRTA*

J.P. Sikora†, Y. Li, CLASSE, Ithaca, New York 14853 USA
S. De Santis, LBNL, Berkeley, California 94720 USA

Abstract

The electron cloud (EC) density in accelerator beam-pipe has been measured using resonant microwaves. The resonances are produced by changes in beam-pipe geometry that generate reflections and standing waves, with typical behavior being similar to a section of waveguide with shorted ends. The technique uses fact that the EC density will shift the resonant frequencies. In previous analysis, we have made the simplifying approximation that the standing waves are multiples of a half-wavelength and that the magnitude of the electric field is symmetric about the longitudinal center of the resonance. In this paper we show that some changes in beam-pipe geometry will result in asymmetric electric field magnitudes along the resonant length. When this is combined with an EC density that varies along this length, the magnitude of the frequency shift will be altered. We present our initial attempt to correct for this effect by modeling the existing beam-pipe using CST Microwave Studio® to obtain a more realistic electric field distribution. This correction is then applied to data taken with beam at several resonant frequencies. The measurements were made at the Cornell Electron Storage Ring (CESR), which has been reconfigured as a test accelerator (CESRTA) providing electron or positron beams ranging in energy from 2 to 5 GeV.

INTRODUCTION

The resonant microwave technique for measuring electron cloud (EC) density has been developed at Cornell over the past several years. Beam-pipe resonances are produced by microwave reflections – a common source being the longitudinal slots at the location of ion pumps, which interrupt the transverse currents of TE waves. The resonant response is obtained by coupling microwaves in/out of the beam-pipe using beam position monitor (BPM) buttons. The measurement technique uses the fact that the beam-pipe's natural frequency ω_0 will be shifted an amount $\Delta\omega$ by the presence of an electron cloud density n_e according to Eq. 1, where E_0 is the magnitude of the resonant electric field, e and m_e are the charge and mass of an electron, ε_0 is the vacuum permittivity and V the resonant volume.

$$\frac{\Delta\omega}{\omega_0} \approx \frac{e^2}{2\varepsilon_0 m_e \omega_0^2} \frac{\int_V n_e E_0^2 \, dV}{\int_V E_0^2 \, dV} \tag{1}$$

An outline of the technique is given in Ref. [1]. In that initial presentation, the simplifying assumption is made that the EC density n_e is uniform over the resonant volume. Equation 1 shows that under these conditions, the resonant field does not need to be known, since the integrals will cancel.

A model for the beam-pipe is a section of waveguide with its ends shorted. The resonant frequencies correspond to m half wavelengths with an envelope $E_0 sin[m\pi(z/L)]$, where m is an integer ≥ 1, z is the location along the beam-pipe and L is the length of the resonant section. This will have resonances at frequencies given by

$$f^2 = f_c^2 + (mc/2L)^2 \tag{2}$$

with f_c the waveguide cutoff frequency and c the speed of light. There is one location, 43E in CESR, where the measured response follows Eq. 2 reasonably well. At that location there is a set of BPM buttons between two ion pumps (with longitudinal slots) and no other changes in geometry. Using Eq. 2, the cutoff frequency f_c of the CESR aluminum beam-pipe extrusion was determined to be 1.8956 GHz. However elsewhere in the storage ring, the beam-pipe resonances do not match this series of frequencies very well. Figure 1 shows the physical layout at the location 15E in CESR, along with the beam-pipe response. The triangles at the top of the plot show the resonant frequencies expected based on the 1.8956 GHz cutoff frequency of the extrusion and the 2820 mm distance between the ion pumps. The larger dark triangle is the cutoff frequency f_c. Dotted lines on the plot connect the observed resonances with the frequencies expected with a shorted waveguide. The first resonance is well below the beam-pipe cutoff frequency.

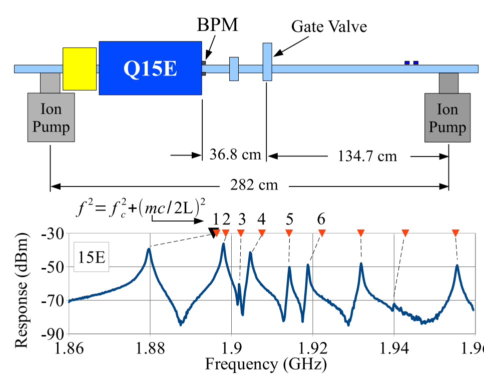

Figure 1: Sketch of the beam-pipe section at 15E along with its resonant response. Triangles show the predicted frequencies for a simple shorted waveguide. Dotted lines connect those frequencies with the measured response peaks.

* This work is supported by the US National Science Foundation PHY-0734867, PHY-1002467 and the US Department of Energy DE-FC02-08ER41538, DE-SC0006505.
† jps13@cornell.edu

ISBN: 978-3-95450-168-7 doi:10.18429/JACoW-IPAC2015-MOPWI031

Inconsistency of Measured Data

Using the technique described in Ref. [1], the EC density at 15E was measured with a 10-bunch train of 5 GeV positrons as a function of beam current using five beam-pipe resonances. Figure 2 shows that there is a disagreement in the measured density of about 25% between the different modes where 15E*m* corresponds to mode *m*. A more recent analysis makes an estimate of the change in EC density along the resonant length by making it proportional to the flux of synchrotron radiation [2, 3], but this had a similar inconsistency between the measurements. There are other parameters that affect the scaling of the measurements, such as the measured Q of each mode, but the expected errors in these parameters are not large enough to explain the data.

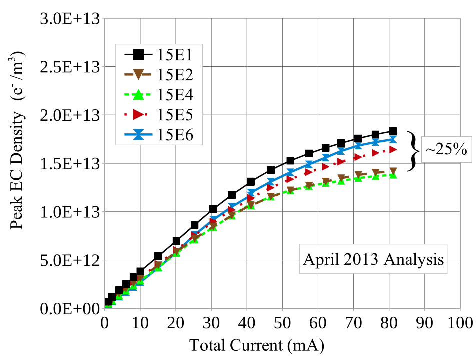

Figure 2: Data from the 15E section of CESR, showing an inconsistency of about 25% in the EC density measurements between the five modes in the same chamber. The label 15E*m* corresponds to mode *m*.

MICROWAVE MODEL OF BEAM-PIPE

The previous section describes two inconsistencies in the analysis of data at 15E: the resonant frequencies do not match the simple model of a shorted waveguide and the EC density versus current measurements do not agree between the different modes. Anticipating that the two are connected, the interior of the beam-pipe at 15E was modeled. First, a model was obtained for the CESR beam-pipe extrusion, then the geometry of the gate valve was added to this model in order to obtain an approximation for the 15E section. Models are created using Autodesk® Inventor™, exported to SAT files, which are then imported into CST Microwave Studio® and the lowest frequency eigenmodes simulated.

Beam-pipe as a Waveguide

The measured series of resonant frequencies at 43E matches that of a shorted waveguide 1385 mm long with a cutoff frequency of 1.8956 GHz. A model was created in Inventor using the dimensions of the drawing for the aluminum extrusion cross-section where the half-width to the beam-pipe wall is 45.009 mm. When this was imported into Microwave Studio®, the simulated cutoff frequency was lower than the measurement by about 1%. A sample

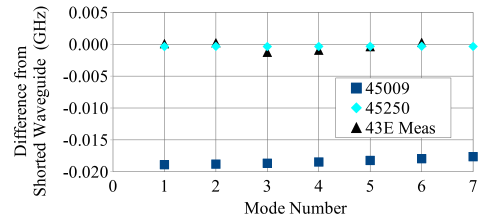

Figure 3: Comparing simulation results of two beam-pipe cross-sections and the measured response peaks at 43E. Labels are for the half-width to the beam-pipe wall in μm.

of the extrusion was measured with a caliper, which gave corrections to the dimensions of the cross-section of about 0.5 mm. Another model was created from these dimensions. The differences between the frequencies of Eq. 2 and those of the two simulations and the measured response peaks at 43E are shown in Fig. 3. Agreement is better that 1:1000 for the simulation based on the measured extrusion dimensions where the half-width to the beam-pipe wall is 45.250 mm.

Beam-pipe with a Gate Valve

Beginning with this model for the beam-pipe, a gate valve was added to create the model for the 2820 mm long 15E section. The gate valve has a recessed region to the outside of the storage ring to avoid synchrotron radiation on the valve body. The dimensions of the recess shown in Fig. 4 are from a model used by the vacuum group. The differences between the frequencies of Eq. 2 and the simulations and the measured data are plotted in Fig. 5. The agreement of the first mode frequency is better that 1:1000 and the other modes agree to within 0.2%. There is a small odd/even disagreement between the measured and simulated frequencies.

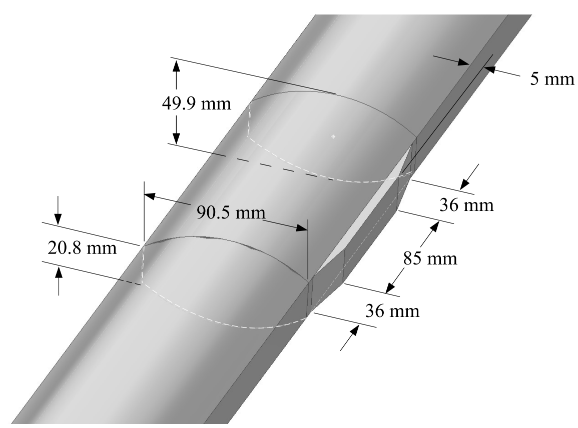

Figure 4: Model created using Inventor with some relevant dimensions. Overall dimensions (above and left) are used in the beam-pipe model. Additional dimensions that model the 5 mm recess of the gate valve body are shown at right.

APPLYING SIMULATION RESULTS

The simulated resonant electric fields for each mode were exported from Microwave Studio®. The square of the elec-

ISBN: 978-3-95450-168-7 doi:10.18429/JACoW-IPAC2015-MOPWI031

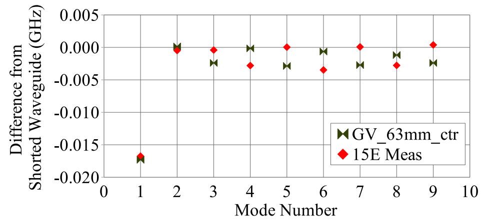

Figure 5: The simulated resonances with the gate valve 63 mm from the longitudinal center are compared with the measured peak frequencies of Fig. 1.

tric field on the beam axis for the relevant modes is plotted in the lower portion of Fig. 6. This shows that the field of the lowest mode is centered at the body of the gate valve. The recess in the gate valve lowers the local cutoff frequency so that the resonance is well below the cutoff frequency of the surrounding beam-pipe and the fields decrease exponentially with distance from the center of the valve. The other modes have a more normal $E_0 sin[m\pi(z/L)]$ appearance, but there is an asymmetry in their amplitude to either side of the gate valve and a reduction in amplitude near the gate valve.

Also plotted in Fig. 6 is an estimate of the relative photon flux based on a SYNRAD simulation [4]. In the absence of external magnetic fields, EC density should be proportional to photon the flux, provided that the flux is low and the beam-pipe material is the same throughout the resonant section. In the presence of an external magnetic field, the EC density will generally be reduced. Figure 6 also contains a plot of an EC multiplier, which is used to scale the EC density for the effects of magnetic field, geometry or material. For this early study the EC multiplier was somewhat arbitrary, with a value that was allowed to vary at the gate valve, and in the region of the quadrupole and sextupole magnets. The magnetic regions were also divided in two parts, near the longitudinal center of the magnets and near their edges.

The product of the SYNRAD photon flux and the EC multiplier is proportional to the EC density. This is then multiplied by E_0^2 and integrated according to Eq. 1 to obtain a correction for the expected frequency shift from the value that is obtained for a uniform density. The data plots are then scaled accordingly.

The EC multiplier was varied using four parameters for the magnetic fields and one for the effect of the gate valve geometry and material until EC density plots for the five modes were close together. The result of this initial optimization is shown in Fig. 7 and is based on the values plotted in Fig. 6. The variation is now only 10% rather than the original 25% seen in Fig. 2.

SUMMARY AND FUTURE WORK

The simulation of resonances in beam-pipe with a gate valve gives electric fields that are asymmetric with respect to the longitudinal center of the resonant section. This has an impact on the sensitivity of particular modes to the details of the EC density along the length of the beam-pipe. An analysis that includes these asymmetric fields along with

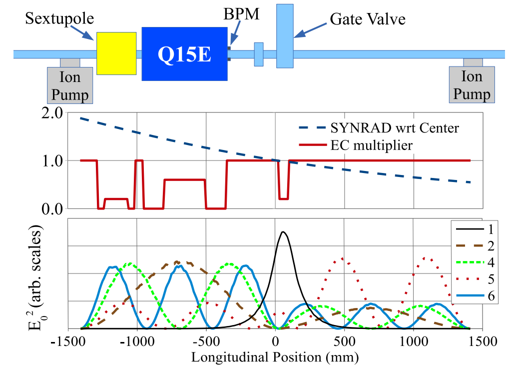

Figure 6: A sketch of the 15E section with the synchrotron radiation flux and the EC multiplier discussed in the text. The lower plots are the values of E_0^2 from simulation of the relevant modes. The scale of mode 1 is altered for clarity.

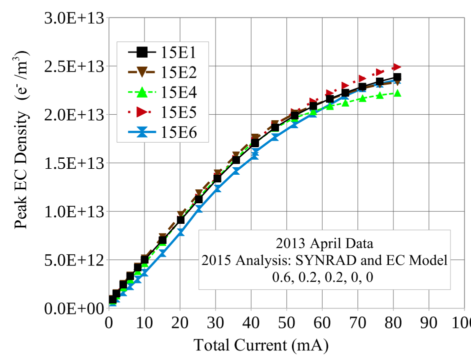

Figure 7: EC density versus beam current with corrections, using the flux, EC multiplier and E_0^2 shown in Fig. 6.

an estimate for the change in EC density along the resonant section, gives plots of EC density versus current that are more consistent with each other. At this level of accuracy, other parameters such as the Q of each mode begin to become important. The inclusion of more mode frequencies in future measurements could yield additional information about the longitudinal distribution of the EC density.

REFERENCES

[1] J.P. Sikora, *et al.*, Nucl. Instrum. Methods Phys. Res., Sect. A **754**, pp. 28-35 (2014), http://dx.doi.org/10.1016/j.nima.2014.03.063, Preprint, arXiv:1311.5633 [physics.acc-ph].

[2] J.P. Sikora, *et al.*, "Electron Cloud Density Measurements Using Resonant Microwaves at CESRTA," in Proc. of IBIC'14, Monterey, CA, USA, September 2014, WEPF21, (2014).

[3] J.P. Sikora, *et al.*, "Cross-calibration of Three Electron Cloud Density Detectors at CESRTA," in Proc. of IBIC'14, Monterey, CA, USA, September 2014, THCXB1, (2014).

[4] D. Sagan, "Design and Applications of the Bmad Library for the Simulation of Particle Beams and X-rays," in *11th International Computational Accelerator Physics Conference, Rostock-Warnemünde, Germany* (2012).